MASTER COPY - FOR REPRODUCTION PURPOSES

2

AD-A210 685 REPORT DOCUMENTATION PAGE

1a. SECURITY CLASSIFICATION AUTHORITY	1b. RESTRICTIVE MARKINGS
2b. DECLASSIFICATION / DOWNGRADING SCHEDULE	3. DISTRIBUTION / AVAILABILITY OF REPORT: Approved for public release; distribution unlimited.
4. PERFORMING ORGANIZATION REPORT NUMBER(S)	5. MONITORING ORGANIZATION REPORT NUMBER(S): ARO 23200.9-LS
6a. NAME OF PERFORMING ORGANIZATION: University of California, Irvine	6b. OFFICE SYMBOL (If applicable)
6c. ADDRESS (City, State, and ZIP Code): Irvine, CA 92717	7a. NAME OF MONITORING ORGANIZATION: U. S. Army Research Office
	7b. ADDRESS (City, State, and ZIP Code): P. O. Box 12211, Research Triangle Park, NC 27709-2211
8a. NAME OF FUNDING / SPONSORING ORGANIZATION: U. S. Army Research Office	8b. OFFICE SYMBOL (If applicable)
8c. ADDRESS (City, State, and ZIP Code): P. O. Box 12211, Research Triangle Park, NC 27709-2211	9. PROCUREMENT INSTRUMENT IDENTIFICATION NUMBER: DAAL03-86-K-0067
	10. SOURCE OF FUNDING NUMBERS: PROGRAM ELEMENT NO. / PROJECT NO. / TASK NO. / WORK UNIT ACCESSION NO.

11. TITLE (Include Security Classification): Excitatory Amino Acids as Transmitters in the Brain

12. PERSONAL AUTHOR(S): Cotman, C.W.

13a. TYPE OF REPORT	13b. TIME COVERED	14. DATE OF REPORT (Year, Month, Day)	15. PAGE COUNT
FINAL	FROM 5/1/86 TO 4/30/89	1989, April 30	39

16. SUPPLEMENTARY NOTATION: The view, opinions and/or findings contained in this report are those of the author(s) and should not be construed as an official Department of the Army position, policy, or decision, unless so designated by other documentation.

17. COSATI CODES		
FIELD	GROUP	SUB-GROUP

18. SUBJECT TERMS (Continue on reverse if necessary and identify by block number): Excitatory receptors, excitatory amino acids, excitotoxicity, N-methyl-D-aspartate, kainate, quisqualate

19. ABSTRACT (Continue on reverse if necessary and identify by block number)

The majority of excitatory transmission in the central nervous system is mediated by excitatory amino acids and their receptors. These receptors participate in both standard synaptic transmission as well as higher order processes such as plasticity and excitotoxicity. In the present report we have carried out detailed biochemical characterization of the different classes of excitatory amino acid receptors. Specific and quantitative binding and autoradiographic assays were developed for purified membrane preparations and thin tissue slices, respectively. These techniques were used to examine and quantify the anatomical distribution and pharmacological properties of each receptor type in the rat brain. There was a high degree of correlation between the results of the biochemical experiments and previously known electrophysiological

20. DISTRIBUTION / AVAILABILITY OF ABSTRACT: ☐ UNCLASSIFIED/UNLIMITED ☐ SAME AS RPT. ☐ DTIC USERS	21. ABSTRACT SECURITY CLASSIFICATION: Unclassified
22a. NAME OF RESPONSIBLE INDIVIDUAL	22b. TELEPHONE (Include Area Code) / 22c. OFFICE SYMBOL

DD FORM 1473, 84 MAR — 83 APR edition may be used until exhausted. All other editions are obsolete.

SECURITY CLASSIFICATION OF THIS PAGE: UNCLASSIFIED

properties, establishing the validity of the binding assays. NMDA (N-methyl-D-aspartate) and QA (quisqualate) receptors exhibited very similar distributions, while KA (kainate) receptors displayed a distribution complimentary to that of the NMDA receptors. Thus, in area such as the mossy fiber pathway of the hippocampus, NMDA receptor density was low, but KA receptor density was high. This distribution was also consistent with the demonstration that long term potentiation (LTP) in this pathway is not blocked by NMDA anatgonists that effectively prevents LTP in NMDA receptor rich pathways. Comparisons of electrophysiological and biochemical properties also indicated that chloride-dependent glutamate binding in the rat brain is not indicative of a specific receptor, but instead represents the binding of L-glutamate to a novel transport system. Further studies also demonstrated that this binding site (and therefore the transport system) is also present on astrocyte membranes. More detailed experiments on the NMDA receptor indicated that this receptor population is not homogeneous, but is most probably comprised of several different subtypes of NMDA receptor. Evidence suggests that glycine, an allsoteric activator of the NMDA receptor, may be involved in the interconversion of these subtypes. Comparative pharmacological studies on the NMDA, QA and KA receptors also identified the non-NMDA receptors as a primary site of action of the exogenous neurotoxin β-N-oxalyl-α,β-diaminopropionic acid. These results illustrate that non-NMDA receptors can also participate in excitotoxic mechanisms.

EXCITATORY AMINO ACID RECEPTORS IN THE BRAIN

The overall goal of this work was to carry out an indepth study of the properties of the excitatory amino acid neurotransmitter receptors. These receptor represent an integral part of the central nervous system, as they are responsible for the majority of the excitatory synaptic transmission, as well as being involved in higher order processes such as plasticity and excitotoxicity. Considerable advances have been made in our understanding of these receptors during the funding period (5/1/86 - 4/30/89). The results of these studies are summarized below with respect to each of the receptor classes.

Excitatory Amino Acid Receptor Distribution:

Quantitative procedures for radioligand binding in membrane preparations and brain slice autoradiography have been developed that allow each of the three excitatory amino acid receptor classes [i.e., N-methyl-D-aspartate (NMDA), kainate (KA), and quisqualate (QA)] to be selectively studied. Thus, each of the receptor subtypes can be individually examined by controlling the radioligand used, buffer makeup and pH, and assay temperature and time. These procedures have allowed the biochemical properties and anatomical distributions of each class to be examined in detail.

The distributions of the excitatory amino acid receptors, as determined by radioligand autoradiography, are shown in the figures below. Color autoradiograms can be found in the original publication (Cotman et al., 1987). In the figure shown, the areas in white represent higher levels of receptor density. Although all of the receptors exhibit a greater density in cortical regions, each has a distinctive distribution.

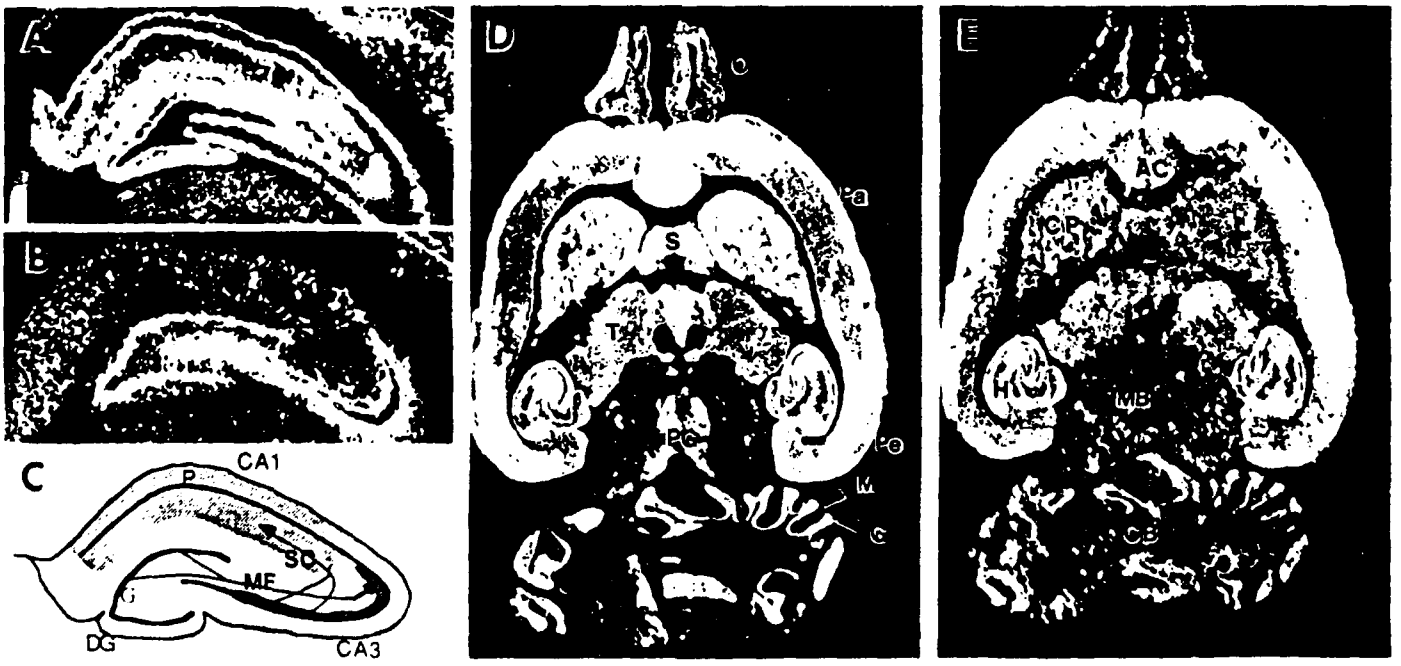

Fig. 1. *Distribution of excitatory amino acid binding sites in rat brain. Binding site density is color-coded with high-to-low densities represented by red-yellow-green-blue. In the hippocampus, high concentrations of NMDA-sensitive [^{3}H]L-glutamate binding sites* (**A**) *are found in CA1 in the termination zone of the Schaffer-collateral/commissural pathway, while high concentrations of kainate-sensitive [^{3}H]L-glutamate binding sites* (**B**) *are found in the terminal field of the mossy fiber (MF) pathway. Schaffer collateral (SC) pathway projecting from CA3 to CA1 is shown in* (**C**) *with its termination zone represented by light hatching. The pathway of the dentate granule cell axons, the mossy fibers (MF), which project to CA3 and its termination zone (stratum lucidum - heavy hatching) is also shown.* (**D–H**) *Horizontal sections of rat brain showing binding sites for* (**D**) *NMDA-sensitive [^{3}H]L-glutamate (agonist binding),* (**E**) *[^{3}H]CPP (antagonist binding),* (**F**) *[^{3}H]kainate;* (**G**) *[^{3}H]glycine (allosteric NMDA potentiator site), and* (**H**) *[^{3}H]TCP (non-competitive antagonist binding site). Abbreviations. P, pyramidal cell layer, DG, dentate gyrus, SC, Schaffer collateral pathway, MF, mossy fiber pathway, G, granule cell layer; O, olfactory bulb; Pa, parietal cortex; Pe, perirhinal cortex, PG periaqueductal gray, S, septum, T, thalamus, M, molecular layer, CP, caudate/putamen; AC, anterior cingulate cortex, H, hippocampus, MB, midbrain, CB, cerebellum.* [Autoradiograms prepared as described in Refs 7(A and B), 9 (D), 17 (E), 33 (F), 65 (H), and Monaghan et al. unpublished (G)]

The distributions of the NMDA and QA receptors were found to be the most similar, suggesting these two receptor may represent a functional combination that is present at a majority of excitatory synapses. KA receptors (studied with ^{3}H-KA), on the other hand, were found to exhibit a distribution that is complimentary to that of the NMDA and QA receptors. Thus, in cortical regions low in NMDA and QA receptors, KA receptors may represent the prominent functional excitatory receptor type.

Correlation of Biochemical and Electrophysiological Studies:

Importantly, the results of the autoradiographic studies correlate very well with electrophysiological studies. For example, NMDA and QA receptors were found to be of greatest density in the CA1 region of the hippocampus. This correlates with both the role of NMDA receptors in long term potentiation (LTP) in this region and the susceptibility of this region to NMDA mediated excitotoxic death. In contrast to region CA1, the mossy fiber pathway of the rat hippocampus exhibited a low the density of NMDA receptors and a high density of KA receptors. Interestingly, electrophysiological studies demonstrated that LTP in this pathway could not be blocked by the NMDA antagonists that were effective in blocking LTP in NMDA receptor-rich pathways.

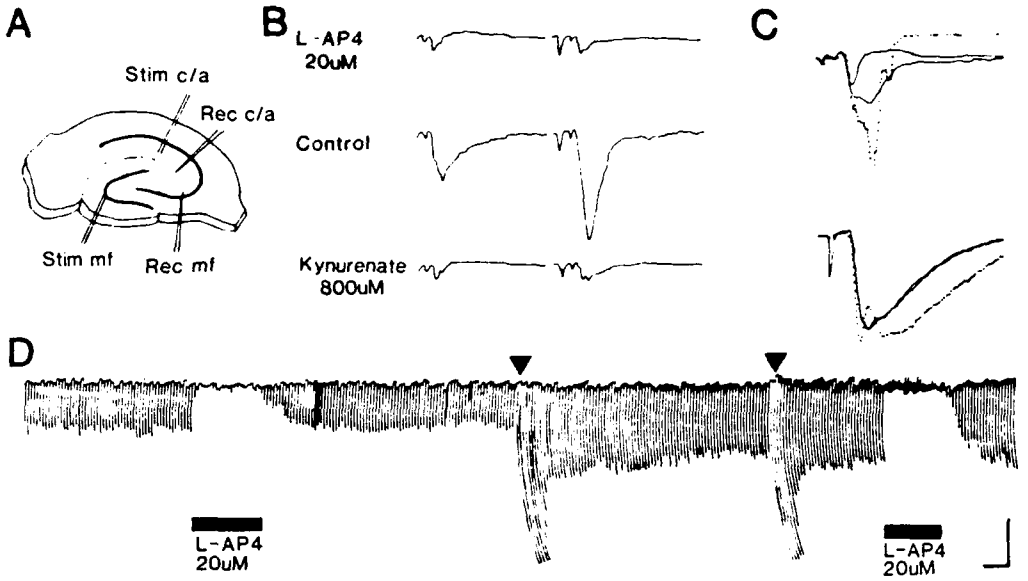

Fig. 1. Mossy fiber and commissural associational responses and induction of LTP. A: electrode positions for stimulating and recording commissural associational and mossy fiber responses. B: tracings of averaged ($n = 4$) mossy fiber responses, showing paired-pulse potentiation at 80-ms interpulse interval (upper, 20 μM L-AP4; middle, after washout; lower, 800 μM kynurenate). C: average of mossy fiber responses (upper) and commissural associational responses (lower) from another slice; responses before and with 20 μM L-AP4 (solid traces), are superimposed on responses taken after washout of L-AP4 and induction of LTP (dotted traces). In the presence of L-AP4, there is still a prominent mossy fiber volley potential. Note also the prominent positive potential following the potentiated mossy fiber response (clipped by the amplifier), reflecting a potentiated commissural associational response not apparent in the control traces. D: polygraph record of mossy fiber response amplitude at a fixed time after each stimulation at 1/20 s. L-AP4 was present during the intervals indicated by the bars. High-frequency stimulation (100 Hz, 100 pulses, 3 times) was delivered at the times indicated by arrowheads. (Calibration: upper, 5 ms, 0.4 mV; lower, 2 min, 0.5 mV.)

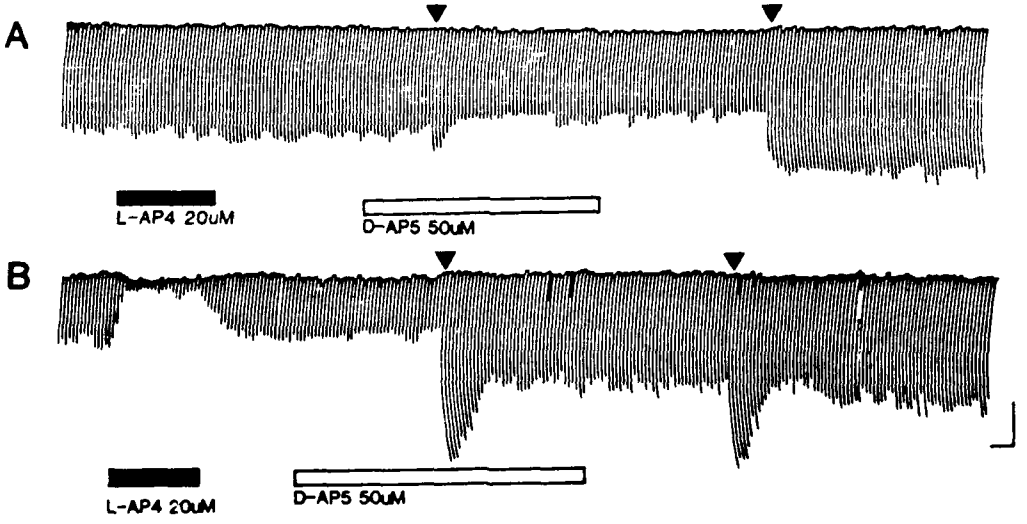

Fig. 2. Effects of D-AP5 on induction of LTP. L-AP4 or D-AP5 were present during the intervals indicated by bars. High-frequency stimulation as delivered at the times indicated by arrowheads. The commissural associational response (A) is insensitive to L-AP4, but the induction of commissural associational LTP is completely blocked by D-AP5. In contrast, mossy fiber responses (B) are profoundly reduced by L-AP4, and although there is a slight effect of D-AP5 on mossy fibers responses (see text), induction of LTP is not blocked by D-AP5. (Calibration: top, 2 min, 0.5 mV; bottom, 2 min, 0.3 mV.)

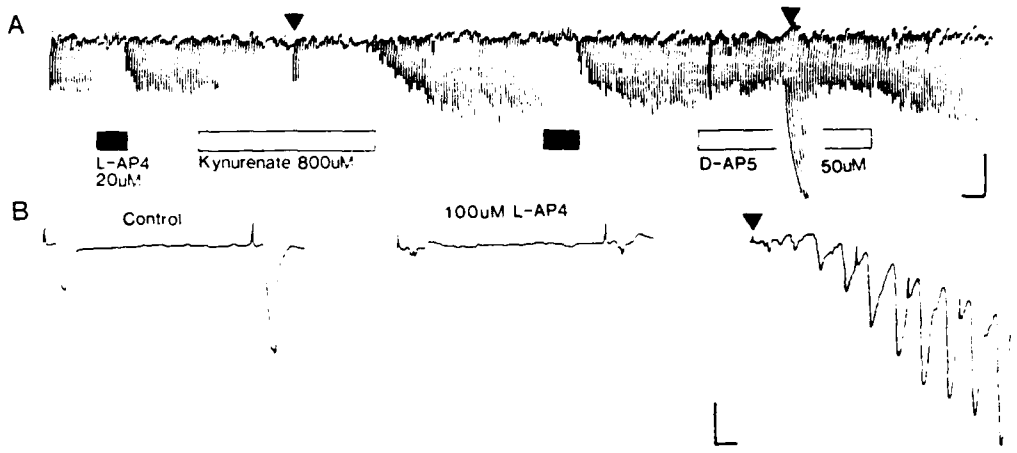

Fig. 3. Mossy fiber potentiation during antagonism by kynurenate and L-AP4. A: both a short term and a lasting increase in response amplitude were produced by high-frequency stimulation in the presence of a concentration (800 μM) of kynurenate that profoundly reduced mossy fiber responses. The lasting increase is best seen by comparing response amplitude before and after kynurenate. The response was again checked for sensitivity to L-AP4 after the first high-frequency stimulation. Little further response increase was produced by a second high-frequency stimulation (delivered in the presence of D-AP5 to prevent induction of commissural associational responses). B, single traces showing antagonism by L-AP4 of mossy fiber responses and paired-pulse potentiation at 80 ms, but not of frequency potentiation during a high-frequency train (100 Hz). (Calibration: top, 2 min, 0.4 mV; bottom, 5 ms, 0.4 mV.)

These results not only indicate there may be more than one type of LTP (e.g., NMDA and non-NMDA), but also suggest that KA receptors might be involved in this process. Thus in addition to anatomic information, the autoradiographic studies are serving an important predictive role in understanding the function of these receptors.

NMDA Receptor Heterogeniety:

More detailed biochemical studies on the NMDA receptor in both membrane and autoradiographic preparations have revealed that this receptor population is not homogeneous, but may actually include several different subtypes of the receptor. This heterogeniety was discerned through detailed pharmacological characterizations that identified an "agonist" and "antagonist" preferring NMDA site. These two different subtypes of NMDA receptors also exhibit distinctive distributions. More recent studies suggest that these forms may be interconverted by glycine, an amino acid that has been shown in electrophysiological studies to be an allosteric activator of the NMDA receptor.

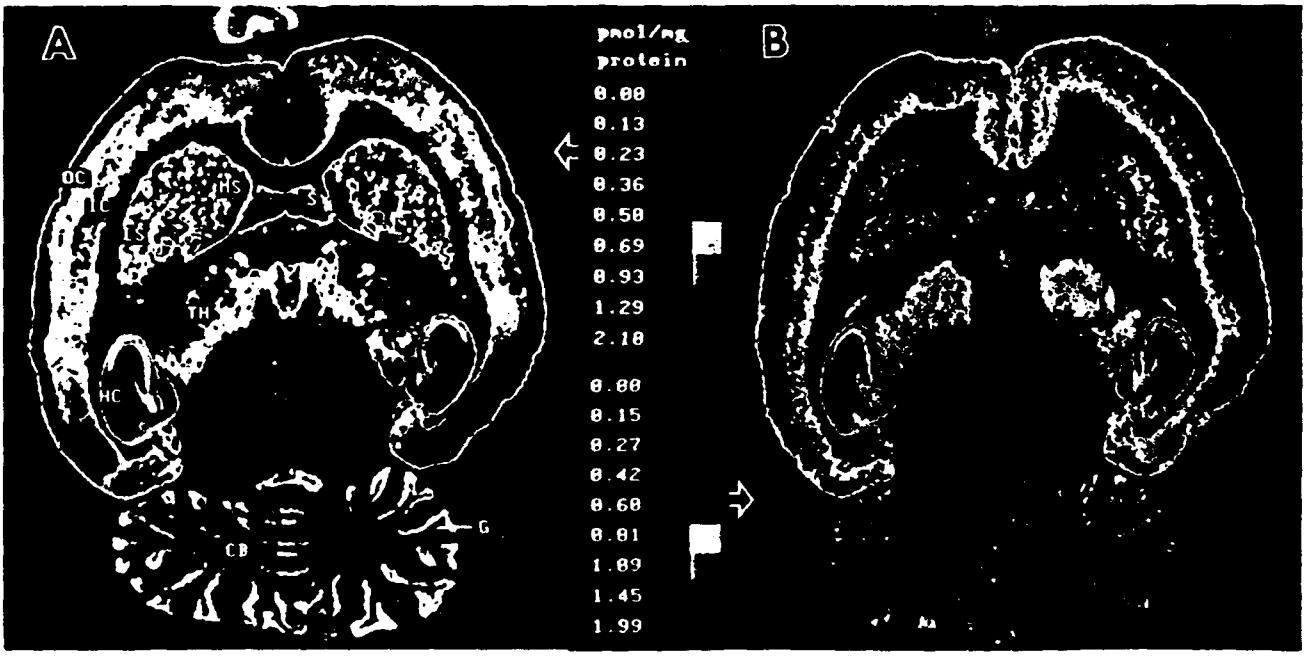

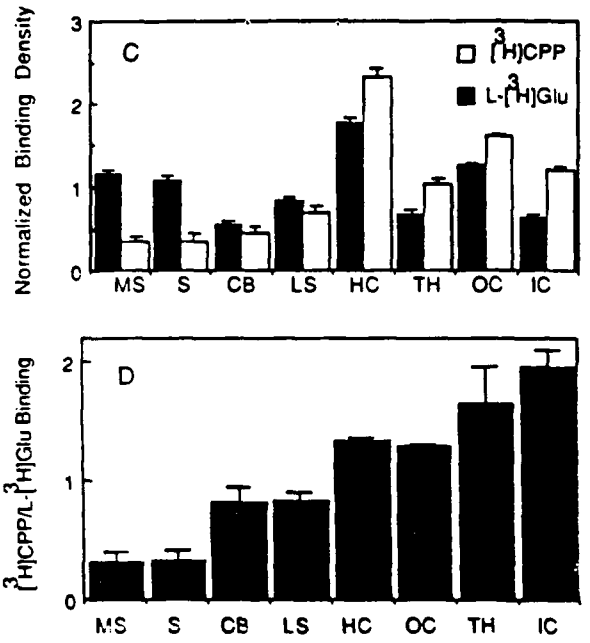

FIG. 1. *Differing distributions of* NMDA receptors in a horizontal plane of the rat brain as determined with the radioligands L-[^{3}H]glutamate (*A*) and [^{3}H]CPP (*B*). Digital images of binding site density are color coded with high-to-low densities represented from red-yellow to green-blue. (*C*) Quantitative values from these experiments. To compare ligands each regional binding value was divided by the average binding level from the eight regions shown. Average L-[^{3}H]glutamate binding was 0.91 ± 0.13 pmol/mg of protein; average [^{3}H]CPP binding was 0.59 ± 0.17. (*D*) The mean [^{3}H]CPP/L-[^{3}H]glutamate normalized binding ratios ± SEM (among animals; n = 4). HC, hippocampus; MS, medial striatum; LS, lateral striatum; S, septum; CB, cerebellar granule cell layer; TH, thalamus; OC, outer (I–III) parietal cortex; IC, inner (IV–VI) parietal cortex; and G, granule cell layer.

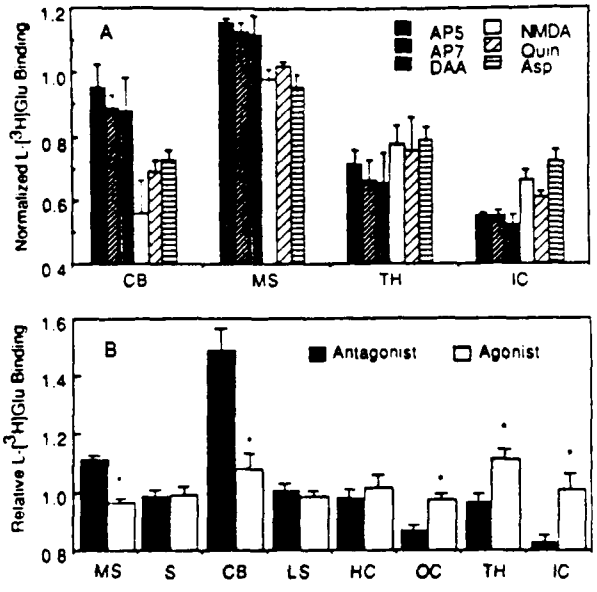

FIG. 2. NMDA-sensitive L-[^{3}H]glutamate binding sites display a regional variability in their sensitivity to NMDA agonists and antagonists. (*A*) L-[^{3}H]Glutamate binding density in the cerebellum, medial striatum, lateral thalamus, and inner parietal cortex measured in the presence of the indicated compounds is expressed as the fraction of average tissue-binding density levels for the same autoradiogram (specified regional binding density divided by average binding density). Average NMDA-displaceable L-[^{3}H]glutamate binding in the absence of displacers was 1.23 ± 0.18 pmol/mg of protein; average displacement was 57.7 ± 5.2%. NMDA antagonists were D-AP5 (AP5; 2.4 μM), 2-amino-7-phosphonoheptanoate (AP7; 11 μM), and D-α-aminoadipate (DAA; 13 μM). NMDA agonists were NMDA (5 μM), L-aspartate (Asp; 5 μM), and quinolinate (Quin; 90 μM). (*B*) *Normalized binding* (as in *A*) is expressed relative to binding in the absence of displacers. Values > 1 indicate that a drug was a weaker displacer in the indicated region than in other regions [*, P < 0.005 for difference between agonists and antagonists by Fisher probable least square difference (PLSD), difference in each region also significant by Scheffé F test]. Abbreviations in legend to Fig. 1.

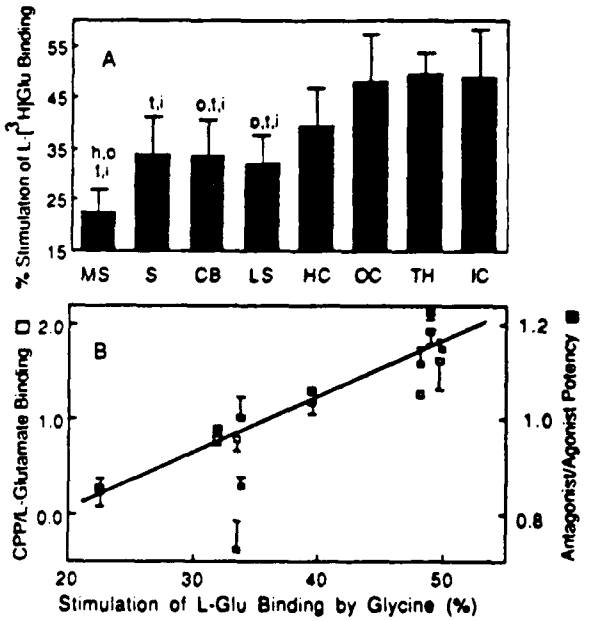

FIG. 3. Glycine enhancement of NMDA-displaceable L-[^{3}H]-glutamate binding sites in tissue sections exhibits a regional variation. (*A*) Mean percent stimulation of L-[^{3}H]glutamate binding by 1 and 10 μM glycine. Similar results were obtained at both concentrations (Fig. 4*A*). Statistically significant (Fisher PLSD, P < 0.05) differences between regions are as compared with the hippocampus (*h*), outer parietal cortex (*o*), lateral thalamus (*t*), and inner parietal cortex (*i*). (*B*) Regional distribution of the percent stimulation by glycine is compared with the distribution of the ratio of [^{3}H]CPP/NMDA-displaceable L-[^{3}H]glutamate binding sites (Spearman correlation coefficient r = 0.89 and without cerebellum r = 0.92) and to the ratio of antagonist to agonist displacement potency (r = 0.88 and without cerebellum r = 0.96). The two antagonist/agonist measures were also correlated (r = 0.88 and without cerebellum r = 0.96). Abbreviations in legend to Fig. 1.

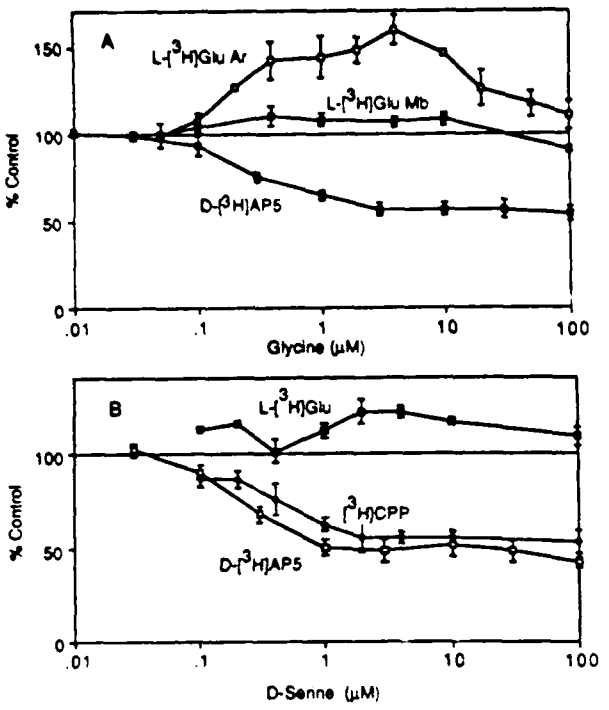

FIG. 4. Differential effect of glycine and D-serine upon NMDA-sensitive L-[^{3}H]glutamate, D-[^{3}H]AP5, and [^{3}H]CPP binding sites in rat brain. (*A*) Glycine enhanced the binding of NMDA-sensitive L-[^{3}H]glutamate binding to extensively washed membrane fractions (Mb) and to whole brain tissue sections (Ar), whereas it potently inhibited 47 ± 4% of the D-[^{3}H]AP5 binding with an IC_{50} = 0.35 μM. (*B*) Similarly, D-serine enhanced NMDA-sensitive L-[^{3}H]glutamate binding in membranes, whereas it maximally inhibited 58 ± 5% of the D-[^{3}H]AP5 binding and 55 ± 5% of the [^{3}H]CPP binding, with IC_{50} = 0.32 ± 0.11 μM and 0.49 ± 0.11 μM, respectively.

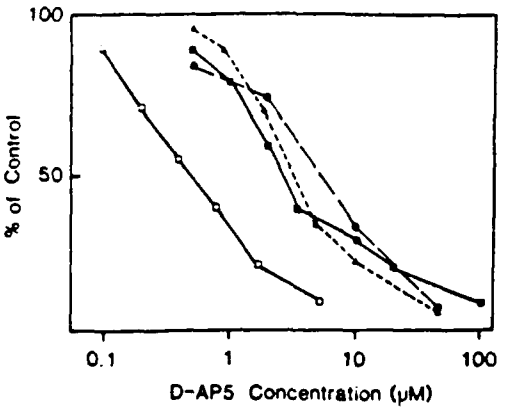

FIG. 5. The different potencies of D-AP5 displacement of agonist (L-[^{3}H]glutamate) and antagonist (D-[^{3}H]AP5) binding (16, 17, 21) are compared with D-AP5 potency at blocking NMDA-induced focal depolarizations and NMDA-receptor-mediated long-term potentiation (28). All measurements were made in the stratum radiatum of CA1 hippocampus. ▲, Long-term potentiation; ●, NMDA depolarization; ■, L-[^{3}H]glutamate binding; and □, D-[^{3}H]AP5.

We currently hypothesize that these subtypes of receptors represent different functional states (i.e., active and inactive) and the ability to distinguish between them will provide important information on the functional status of the receptors.

Chloride-Dependent Glutamate Binding Represents a Transport System

An important aspect of investigating the excitatory amino acid receptors and a goal of the proposal concerns establishing that the binding procedures used actually represent the interaction of ligands with physiologically relevant receptors. In this regard, the mere presence of a "binding" site does not necessarily mean that the ligand is binding to a transmitter receptor, as ligands can also bind specifically to other enzymes or transport systems. In the present studies we have shown that the procedures used to examine NMDA, KA and QA receptors do, indeed, represent receptor binding. This is best illustrated by the excellent correlation between binding experiments and electrophysiological studies. In contrast to these finding, however, we have found that the majority of ^{3}H-L-glutamate bound to synaptic plasma membranes in the presence of chloride ions actually represents the interaction of glutamate with an uptake system and not a transmitter receptor.

TABLE 1. *Types of glutamate binding sites on astrocyte membranes*

Experiment	Ligand	Assay buffer	Bound (pmol/mg protein)	Percent of maximum
1	[^{3}H]KA	Tris-citrate	ND	—
2	[^{3}H]AMPA	Tris-acetate	ND	—
3	L-[^{3}H]Glutamate	Tris-Cl and calcium	7.36 ± 1.9	100
4	L-[^{3}H]Glutamate	Tris-Cl	6.91 ± 0.4	94 ± 5
5	L-[^{3}H]Glutamate	Tris-acetate	0.72 ± 0.4	10 ± 5
6	L-[^{3}H]Glutamate	Tris-acetate and calcium	0.96 ± 0.3	13 ± 3

Astrocyte membranes were assayed for [^{3}H]KA (10 n*M*), [^{3}H]AMPA (50 n*M*), and L-[^{3}H]glutamate (100 n*M*) by the assay procedures described in Materials and Methods. Values indicated represent specific binding. ND, not detected.

TABLE 2. *Ligand specificity of Cl^--dependent binding in astrocyte membranes*

Compound	Percent of control
None	100
L-Aspartic acid	4 ± 3
L-Cysteic acid	11 ± 6
L-α-Aminoadipic acid	24 ± 6
Cysteine sulfinic acid	29 ± 8
Quisqualic acid	49 ± 2
L-Homocysteic acid	58 ± 6
D-Glutamic acid	64 ± 5
D-Aspartic acid	76 ± 6
2-Amino-5-phosphonopentanoate	84 ± 6
2-Amino-6-phosphonohexanoate	86 ± 11
KA	86 ± 11
AP4	95 ± 15
AMPA	106 ± 11
NMDA	106 ± 26

Astrocyte membranes were assayed for Cl^--dependent L-[^{3}H]glutamate (100 n*M*) binding as described in Materials and Methods (50 m*M* Tris-Cl, 1 m*M* Ca^{2+}, pH 6.9, 60 min, 30°C). Glutamate analogues were included at 100 μ*M*. Calculated values are all based on specific binding.

TABLE 3. *Inhibition of Cl^--dependent glutamate binding in astrocyte membranes*

Experimental conditions	Percent of control
1. Control	100
2. SITS (1 m*M*)	12 ± 2
3. DIDS (1 m*M*)	11 ± 3
4. Furosemide (1 m*M*)	22 ± 5
5. Sodium-acetate (5 m*M*)	90 ± 5
6. Frozen/thawed	104 ± 5
7. 0–4°C Assay	17 ± 7

Astrocyte membranes were assayed for Cl^--dependent L-[^{3}H]glutamate (100 n*M*) binding as described in Materials and Methods (50 m*M* Tris-Cl, 1 m*M* Ca^{2+}, 60 min, 30°C). The listed compounds were included at the concentrations indicated. Samples in Expt. 6 were frozen and thawed at least three times. Calculated values are all based on specific binding.

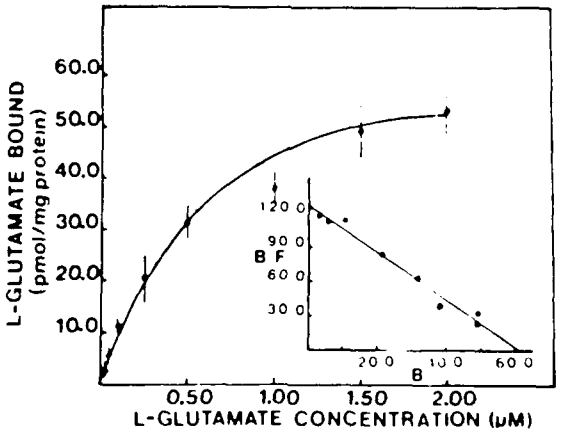

FIG. 1. *Cl*$^-$*-dependent binding to astrocyte membranes* is shown as a function of glutamate concentration. The values represent the means ± standard deviations of specific binding from a representative experiment. A Scatchard analysis of these data is presented in the inset. Assays were performed as described in Materials and Methods (50 m*M* Tris-Cl, 1 m*M* Ca^{2+}, pH 6.9, 60 min, 30°C)

Furthermore, this uptake system is present on astrocytes and can be studied in membranes prepared from cultured astrocytes. Thus, these studies have not only helped to identify a novel transport system, but they have also clarified the complications introduced into other binding studies by the inclusion of chloride ions.

Exogenous Neurotoxins Can Act at Non-NMDA Receptors

Biochemical studies on the QA receptor have shown that this receptor has a high affinity for the glutamate analogue, β-N-oxalyl-L-α,β-diaminopropionic acid (β-L-ODAP). In contrast to this high affinity, this derivative is a very weak inhibitor of NMDA receptor binding. This is particularly interesting because β-L-ODAP is a known neurotoxin that produces a permanent spastic paralysis upon excessive consumption of the seeds that contain the toxin. Thus, as the concentration of the toxin in the CNS increases, we would predict that the first excitatory receptor system to be effected would be the QA type.

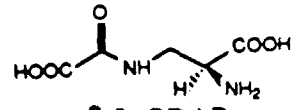

β-L-ODAP
(β-N-Oxalyl-L-α,β-diamino-propionic acid)

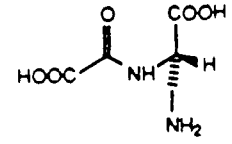

α-L-ODAP
(α-N-Oxalyl-L-α,β-diamino-propionic acid)

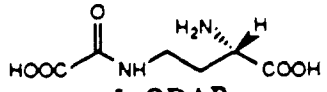

γ-L-ODAB
(γ-N-Oxalyl-L-α,γ-diamino-butyric acid)

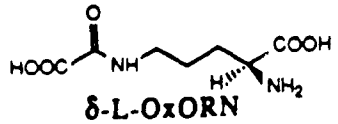

δ-L-OxORN
(δ-N-Oxalyl-L-ornithine)

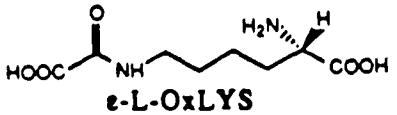

ε-L-OxLYS
(ε-N-Oxalyl-L-lysine)

Table 1. Pharmacological specificity of *N*-oxalyl-diamino-dicarboxylic acids

Compound (conc.)	QA site ^{3}H-AMPA (% control)	KA site ^{3}H-KA (% control)	NMDA site ^{3}H-GLU (% control)
Control	100	100	100
β-L-ODAP			
1 μM	57 ± 5	97 ± 7	96 ± 8
20 μM	8 ± 2	56 ± 4	86 ± 3
100 μM	0 ± 1	29 ± 6	61 ± 9
β-D-ODAP, 100 μM	91 ± 8	87 ± 5	52 ± 6
α-L-ODAP, 100 μM	90 ± 8	97 ± 7	83 ± 10
γ-L-ODAB, 100 μM	83 ± 8	84 ± 9	36 ± 4
γ-D-ODAB, 100 μM	95 ± 7	96 ± 9	40 ± 4
δ-L-OxORN, 100 μM	90 ± 11	94 ± 7	56 ± 4
δ-D-OxORN, 100 μM	104 ± 7	92 ± 3	36 ± 4
ε-L-OxLYS, 100 μM	80 ± 9	89 ± 9	77 ± 8
ε-D-OxLYS, 100 μM	83 ± 10	98 ± 2	41 ± 5

Inhibition of radioligand binding to synaptic plasma membrane excitatory amino acid receptors by *N*-oxalyl-diamino-dicarboxylic acids. QA, KA, and NMDA receptors were selectively assayed with ^{3}H-AMPA (10 nM), ^{3}H-KA (10 nM), and ^{3}H-L-GLU (10 nM), respectively. Details of the assays are described in Materials and Methods. Inhibitors were included in the binding assays at the concentrations indicated. All values represent specific binding and are reported as the averages (n = 5–8) of the percentage of control binding ± SD.

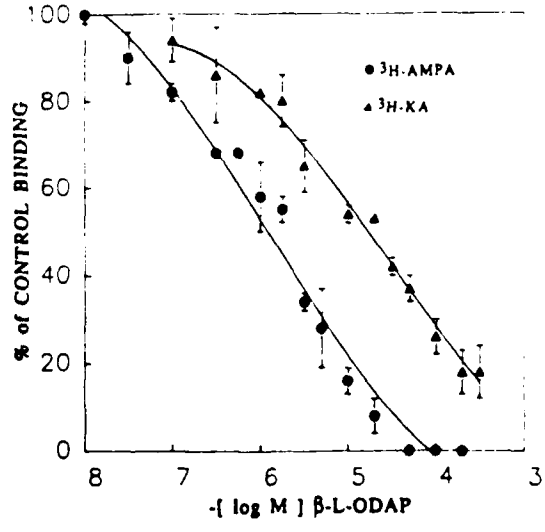

Figure 2. Inhibition of ^{3}H-AMPA and ^{3}H-KA binding by β-L-ODAP. Concentration dependence of the inhibition of (●) ^{3}H-AMPA (10 nM) binding to QA sites and (▲) ^{3}H-KA (10 nM) binding to KA sites by β-L-ODAP. Details of the radioligand binding assays are described in Materials and Methods. The values reported represent percentages of control binding in the presence of inhibitor (means ± SD, n = 5–7) and have been corrected for specific binding. The curves have been fitted by computer as a third-order polynomial. IC_{50} values were calculated to be 1.3 ± 0.2 μM for the inhibition of ^{3}H-AMPA binding and 17.0 ± 2.0 for the inhibition of ^{3}H-KA binding.

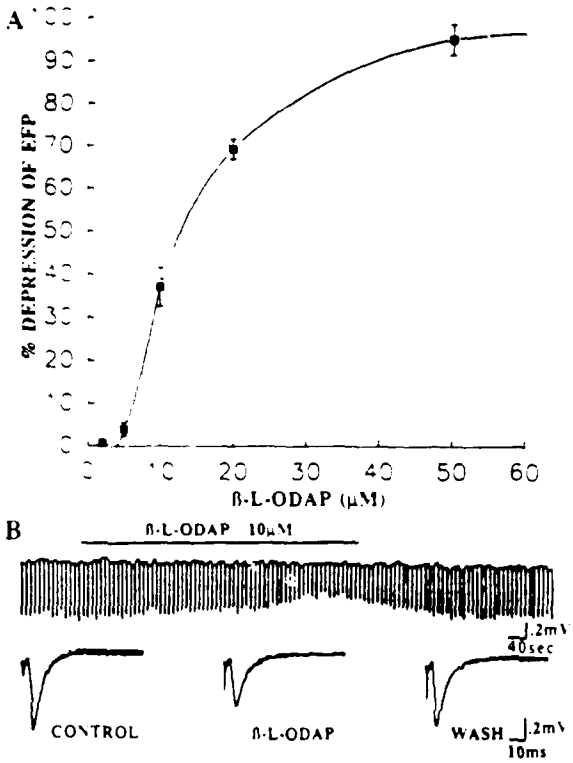

Figure 3. Extracellular records of the effect of β-L-ODAP on synaptic transmission. Application of β-L-ODAP to hippocampal slices depressed the extracellular field potential (*EFP*) recorded in the Schaffer collateral terminal zone of area CA1. *A*, β-L-ODAP depresses the EFPs in a concentration-dependent manner. Each reported value represents the mean percent depression (±SEM) of control EFPs (n = 3–7 trials). The curve was fitted using a packaged cubic spline program. The IC_x value interpolated from the curve for the depression of the EFPs is 12 μM. *B*. Representative records collected during a trial in which β-L-ODAP was applied at a concentration near the IC_{50} are shown. A sample and hold record during the application (*bar*) and subsequent washout of β-L-ODAP illustrates the time course of the EFP depression. The bottom traces are averages of 10 EFPs from the record above. In the trial shown, β-L-ODAP depressed the EFP by 37%.

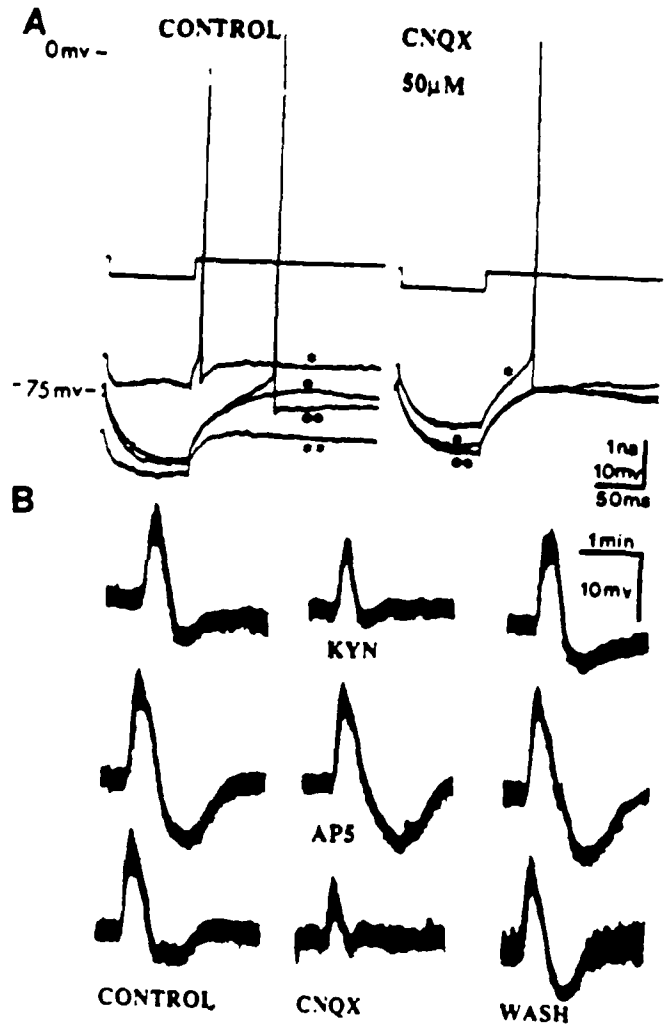

Figure 4. β-L-ODAP-induced depolarization of hippocampal neurons is blocked by non-NMDA antagonists. *A*, Dropwise application of a concentrated solution (1000 μM) β-L-ODAP to hippocampal pyramidal neurons results in depolarization that is accompanied by a large decrease in membrane resistance (★). The control trace (●) demonstrates the original membrane potential and input resistance. Following β-L-ODAP application there was a period of hyperpolarization that was associated with a conductance increase (★★) prior to recovery (●●). Addition of CNQX (50 μM) to the ACSF reduced the conductance increase produced by β-L-ODAP by 60% (n = 2). Current traces are shown in the upper portion of figure. *B*, Records of membrane potentials from the same neuron demonstrate the effects of (1) a nonselective glutamate receptor antagonist, kynurenic acid (*KYN*, 500 μM); (2) a selective NMDA antagonist, AP5 (50 μM); and (3) a non-NMDA antagonist, CNQX (50 μM), on the depolarization induced by the drop application of β-L-ODAP (estimated concentration, 10 μM). In the records shown above, KYN and CNQX depressed the β-L-ODAP-induced depolarization by 37 and 53%, respectively. Membrane potentials returned to normal after each of the drugs was washed out.

Although previous studies have shown that NMDA receptor agonists are potent neurotoxin, the present results now suggests that non-NMDA receptors can also contribute to this neurotoxic process and must be taken into account into the design of any therapeutic approach to prevent excitotoxicity.

Publications:

Harris, E.W. and Cotman, C.W. (1986) Long-term potentiation of the guniea pig mossy fiber responses is not blocked by N-methyl-D-aspartate antagonists, *Neurosci. Lett.* 70: 132.

Bridges, R.J., Nieto-Sampedro, M., Kadri, M., and Cotman, C.W. (1987) A novel chloride-dependent ^{3}H-L-glutamate binding site in astrocyte membranes, J. Neurochem., **48**, 1709.

Bridges, R.J., Kesslak, J.P., Nieto-Sampedro, M., Broderick, J.T., Yu, J., and Cotman, C.W. (1987) A ^{3}H-L-glutamate binding site on glia: an autoradiographic study on implanted astrocytes, Brain Research, **415**, 163.

Cotman, C.W., Monaghan, D.T., Ottersen, O.P., aand Storm-Mathisem, J. (1987) Anatomical organization of excitatory amino acid receptors and their pathways, *Trends in Neurosci.* 10: 273.

Monaghan, D.T.,Cotman, C.W, Olverman, H.J, and Watkins, J.C.(1988) Two classes of NMDA recognition sites: Differential distribution and regulation by glycine, in *Frontiers in Excitatory Amino Acid Research*, ed. E.A. Cavalheiro, J. Lehmann, L. Turski. New York: Liss, 745.

Monaghan, D.T., Olverman, H.J., Nguyen, L., Watkins, J.C., and Cotman, C.W. (1988) Two classes of NMDA recognition sites: Differential distribution and differential regulation by glycine, *Proc. Natl. Acad. Sci. USA* 85: 9836.

Bridges, R.J., Kadri, M., Monaghan, D., Nunn, P.B., Watkins, J.C., and Cotman, C.W. (1988) Inhibition of ^{3}H-α-amino-3-hydroxy-5-methyl-4-isoxazolepropionic acid (AMPA) by the excitotoxin β-N-oxalyl-L-α,β-diaminopropionic acid, Eur. J. Pharmacology, **145**: 357.

Bridges, R.J., Stevens, D.R., Kahle, J.S., Nunn, P.B., Kadri, M., and Cotman, C.W. (1989) Structure-function studies on N-oxalyl-diamino-dicarboxylic acids and excitatory amino acid receptors: evidence that β-ODAP is a selective non-NMDA agonist. J. Neuroscience, **9**: 2073.

Geddes, J.W., Cooper, S.M., Cotman, C.W., Patel, S., and Meldrum, B.S. N-Methyl-D-aspartate receptors in the cortex and hippocampus of baboon (Papio anubis and Papio papio) (submitted).